Journal of Energy Storage 60 (2023) 106652

Contents lists available at ScienceDirect

Journal of Energy Storage

journal homepage: www.elsevier.com/locate/est

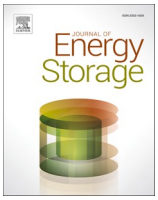

Research papers

Optimizing the discharge process of a seasonal sorption storage system by means of design and control approach

Alicia Crespo [a], Andrea Frazzica [b], Cèsar Fernández [a], Álvaro de Gracia [a,*]

[a] GREiA Research Group, Universitat de Lleida, Pere de Cabrera s/n, 25001 Lleida, Spain
[b] Institito di Tecnologie Avanzate per l'Energia "Nicola Giordano", CNR-ITAE, Messina, Italy

ARTICLE INFO

Keywords:
Seasonal thermal energy storage
Sorption heat storage
Numerical simulations
Solar thermal energy
Performance and control optimization

ABSTRACT

Sorption thermal energy storage systems have higher energy densities and low long-term thermal losses compared to traditional energy storage technologies, which makes them very attractive for seasonal heat storage application. Although they have a lot of potential at material level, its operation and system implementation for residential application requires further study. The performance of a seasonal sorption thermal energy storage system strongly depends on the discharging process during the cold season. The present study analysed through numerical simulations different scenarios to enhance the thermal performance of a solar-driven seasonal water-based sorption storage, which supplied space heating and domestic hot water to a single-family house in a cold climate region. All studied scenarios were analysed under optimal control policy. The results indicated that the sorption storage could increase by 9 % its energy density if conservative and constant discharging temperature set points are considered, due to fewer interruptions during the discharge. The energy density of the sorption storage driven by solar energy was highly impacted by the weather conditions, and by the type and availability of low-temperature heat source. Indeed, the energy density of the sorption storage increased by 22 % using a water tank to assist the evaporator of the sorption storage, instead of a latent storage tank. The use of a dry-heater to assist the evaporator with environmental heat was not suitable for the climate studied due to the low hours of operation. The sorption storage system composed of 20 modules of LiCl-silica gel could obtain an energy density and a COP of 139 kWh/m^3 and 0.39, respectively, if a constant low-temperature heat source (i.e, geothermal or waste energy) was available.

1. Introduction

According to the International Energy Agency (IEA) [1], thermal energy demand in the residential sector accounts for 46 % of the global heat consumption. Thermal energy storage (TES) allows the use of time-discontinuous renewable sources, such as solar energy, to supply the increasing thermal demand at short (days or weeks) or long-term (months) by decoupling the heat source and the thermal demand. Long-term TES systems, commonly called, seasonal thermal energy storage (STES), are employed to store solar thermal energy harvested during the summer period to be discharged during winter, mainly to cover space heating (SH) demand. The main critical parameters to be considered for the design of a suitable seasonal TES among others are [2]: low thermal losses to the ambient during the storage period, high energy density, and low investment costs. There are three classes of TES systems, which can be used as seasonal storage: sensible, latent, and thermochemical systems. Sensible and latent storage systems suffer high-energy losses to the ambient during long storage period, especially in winter; furthermore, they are characterized by limited energy storage density. Therefore, they are not considered a suitable technology for long-term TES applications. Thermochemical TES concept is based on a reversible physical or chemical reaction occurring between two components [3]. One of the most investigated thermochemical TES technologies is the sorption one, since the required charging/discharging temperature levels are suitable for solar thermal collectors and common building SH distribution systems (e.g. underfloor heating, fan coils).

Sorption TES consists of a reversible reaction between a working fluid, often referred as sorbate (e.g. water vapour) and a solid or liquid sorbent medium [4]. During the desorption (charging) the sorbent releases the sorbate (vapour) at regeneration temperature through an endothermic reaction. Heat of sorption is stored as long as the sorbent and the sorbate are kept separated. The sorption (discharging) starts when the sorbent and the sorbate interact again (at the corresponding

* Corresponding author at: GREiA Innovació Concurrent, INSPIRES Research Centre, University of Lleida, Pere de Cabrera s/n, 25001 Lleida, Spain.
E-mail address: alvaro.degracia@udl.cat (Á. de Gracia).

https://doi.org/10.1016/j.est.2023.106652
Received 13 September 2022; Received in revised form 13 December 2022; Accepted 8 January 2023
Available online 20 January 2023

Nomenclature

Symbols

C_p	Specific heat, kJ/kgK
$\dot{m}$	Mass flow rate, kg/h
Q	Thermal power, kW
T	Temperature, °C
U	Thermal transmittance, kJ/hm^{2}K
A	Area, m^2
a_0	Collector's optical efficiency
a_1	First order collector efficiency, W/m^{2}K
a_2	Second order collector efficiency, W/m^{2}K^2
D	Thermal demand, kWh
E	Energy, kWh
e_d	Energy density, kWh/m^3
C	Unitary cost, €/kWh
J	Last time-step
t	Time step
V	Volume, m^3
E_G	Solar irradiation, W/m^2

Subscripts

b	Boiler
out	Outlet
in	Inlet
avg	Average value
ad	Adsorption
de	Desorption
min	Minimum
e	Evaporator
col	Collector
dis	Discharge
c	Condenser
sen	Sensible
sorb	Sorbent material
r	Regeneration
el	Electrical
nosup	Not supplied demand
ch	Charge
S	Summer
W	Winter

Acronyms

SF	Solar fraction
HTF	Heat transfer fluid
SF	Solar fraction
DHW	Domestic hot water
SH	Space heating
COP	Coefficient of performance
GTL	Gross temperature lift
TE	Temperature effectiveness
TES	Thermal energy storage
PCM	Phase change material
RBC	Rule based control
STES	Seasonal thermal energy storage
TAC	Total annual cost
PF	Penalty factor
LTHS	Low temperature heat source
SWS	Selective water sorbents
IAM	Incidence angle modifier

equilibrium temperature and vapour pressure): the sorbate in its gaseous phase penetrates into the solid or liquid sorbent [2]. As long as sorbent and sorbate are kept separated, the thermal losses to the ambient are zero. Moreover, several studies have also reported high energy densities of sorbent materials [5–8]. Hence, sorption TES are very good candidates to work as seasonal TES since they present high-energy density and low heat losses to the ambient during the storage period.

Regardless the heat losses to the ambient during the storage period are zero, seasonal sorption TES consumes thermal energy to heat up the system (sensible heat) as part of the process to reach the desorption or adsorption temperature. Both in summer and winter, heat losses to the ambient between two consecutive discharges entail a decrease in the system energy efficiency and energy density. Despite some studies neglect the thermal losses to the ambient, heat dissipation of reactors cannot be neglected in a real system [9] and they must be accounted to evaluate the key performance indicators of a seasonal sorption TES. That was highlighted by N'Tsoukpoe et al. [10], who concluded that seasonal thermochemical heat storage is subjected to significant thermal losses.

Sorption TES requires a low-temperature heat source (LTHS) to support the evaporator. Ammonia-based systems have the advantage of having high operation pressure and low freezing point of liquid ammonia compared with water-based systems [11]. For this reason, ammonia-based sorption systems usually take profit from ambient air as LTHS during the discharging process in winter. In consequence, the performance of ammonia-based systems directly depends on ambient temperature, especially during cold winter days. This is because the ambient temperature in winter (evaporator inlet temperature) is low, and thus would lead to a decrease in the heat output temperature [12], since lower evaporator inlet temperature decreases the efficiency of the sorption system. Several authors have proposed possible solutions to tackle the impact of low ambient temperatures on the system performance of ammonia-based sorption storage systems. Li et al. [12] presented an innovative dual-mode thermochemical sorption energy storage for seasonal storage. The seasonal storage, charged by solar thermal energy, supplied heat to a radiant floor heating system. The dual mode goaled to enhance the ammonia-based sorption TES during its discharging phase at low ambient temperatures. Indeed, during those days, the sorption system was upgraded with a sorption heat transfer cycle. The authors reported the influence of the ambient temperature in winter on the COP, energy density, and heat production. The results indicated that the lower the ambient temperature, the worst the system performance. In a later study, Li et al. [11] developed and experimentally investigated the feasibility and working performance of the dual-mode thermochemical sorption TES under different ambient temperatures in winter. Other authors also presented solutions to tackle the issue. Jiang et al. [9] investigated experimentally the performance of an ammonia-based resorption (two salts) TES system for seasonal storage. The authors presented the temperature upgrade (internal heat recovery between reactors) and sorption compression mode as possible solutions to overcome extremely low ambient temperatures. Energy density and system efficiency were studied under different conditions of input, output and ambient temperatures (local ambient temperatures from 5 to 15 °C). The authors [9] also analysed the mass ratio between the metal and composite sorbent to evaluate its influence on the system performance.

Jiang continued analysing sorption systems for seasonal heat storage. In a further study [13], the authors analysed the performance of an ammonia-based hybrid compression-assisted sorption TES under severe cold conditions (i.e: −30 °C to −5 °C), under which its operation is affected. The authors considered a photovoltaic-thermal collector: the electricity was used by the compressor and the heat was absorbed by the high-temperature reactor in summer and by the low temperature reactor during cold winter days. Avoiding in the latter case the use of ambient air, since its temperature was very low. The same hybrid sorption

seasonal storage system was analysed for a typical winter and summer day for three cities with ultra-low temperatures [14], concluding that the system was quite promising for severe cold regions. Ma et al. [15] analysed the integration of an electric heater or an electric-driven compressor into a solar-driven seasonal thermochemical sorption system to assist the desorption process when solar energy was not available. The results revealed that the hybrid thermochemical sorption system with a compressor substantially improved the storage capacity compared to the one with electric heater. In addition, Ma et al. [16] analysed the potential of a solar driven seasonal TES system employing different ammonia-based chemisorption materials integrated in UK dwellings. The best scenario, using $BaCl_2$–$0/8NH_3$ (45.2 m^3 storage volume) and 30.5 m^2 solar collectors supplied 57.4 % of a dwelling SH demand.

Water-based sorption storage systems cannot operate when evaporation temperature is below 0 °C [9] due to their freezing point. In spite of having a narrower operation range at the evaporator, water-based systems present several advantages compared to ammonia-based sorption systems: they are not toxic, suitable for floor SH temperatures, and usually require desorption temperatures below 100 °C [17], which allow the use of non-concentrating collectors which present lower investment costs and can be installed in the roof of the dwellings. Moreover, they can achieve higher energy storage density thanks to the higher enthalpy of evaporation of water compared to ammonia.

Bearing in mind the freezing point of water which hinders the use of ambient heat, water-based sorption TES systems require an external heat source to assist the evaporator during cold winter days. Although the operation depends to a lesser extent on the ambient temperature compared to ammonia-based systems, it must also be studied in detail, as Frazzica et al. [18] highlighted the influence of the ambient heat source/sink on seasonal sorption TES. In addition, a sorption system has to be studied not only at the component level under defined boundary conditions [19–21], but also integrated into a building subjected to dynamic weather conditions and thermal demands throughout the year. In a previous work, Crespo et al. [22] optimized the control of a seasonal water-based sorption thermal energy storage coupled to solar collectors. The system supplied domestic hot water (DHW) and SH to a single-family house in middle Europe. The sorption storage system consisted of an asymmetric heat exchanger [23] containing a selective water sorbent (SWS) – LiCl/silica gel [24]. The results proved that the size of the sorption storage system could be reduced by around 10 % obtaining optimal operational annual costs thanks to the control optimization. The authors concluded that further research on the optimization on the availability and outlet temperature of the LTHS must be performed. Engel et al. [25] assessed through simulations a water-based sorption storage coupled to a building heating system located in different locations inside Europe. The authors analysed a modular implementation of the sorption process with operational modes like the “charge boost”, which consisted in the vapour transfer between sorption modules. According to the authors, this novel operational mode allowed to reach a higher state of charge for a given temperature level.

As reviewed, several studies presented solutions to enhance the efficiency of sorption systems during the discharging phase. Nevertheless, the studies focused on ammonia-based sorption systems [11–13,15]. Engel et al. [25] analysed the performance of a water-based sorption storage coupled to a building heating system. Nevertheless, the proposals focused on the charging phase, such as the “charge boost”. Moreover, the authors reported oversizing in some scenarios because the control parameters were not optimized for each scenario. This study aims at improving the competitiveness of a solar-driven seasonal water-based sorption system located in a cold climatic region by proposing possible solutions to enhance the discharging efficiency of the sorption modules. For that purpose, different LTHS and different discharging temperature set points of the sorption modules were explored with annual numerical simulations. Moreover, we step forward in comparison with previous studies by optimizing the control strategy for every scenario to avoid the overestimation of the sorption storage volume. Increasing the efficiency of the sorption TES system is a key factor to push the technology forward and position it as an alternative to other seasonal TES systems (e.g. water tanks, borehole TES).

2. Methodology

This section presents the methodology used in this study. Fig. 1 presents a flowchart with the different steps of the methodology, which is explained in detail throughout this section.

2.1. System and operational description

In this study, a solar-driven seasonal sorption thermal energy system is presented. The system was mainly composed of evacuated tube collectors, a 20-module water-based sorption TES system (STES), a stratified water tank (also called combi-tank), and a backup gas boiler, which supplied SH and DHW to a single-family house. Due to its seasonal behaviour, the system had different operation and configuration during hot and cold seasons, as shown in Figs. 2 and 3, respectively. The main difference between both configurations in terms of system components were the low-temperature heat sources, which were just required during winter to assist the evaporator of the sorption storage system.

The configuration and the operation of the seasonal system were mainly defined based on the performance requirements of the sorption heat storage. The sorbent material of the seasonal sorption TES consisted of LiCl embedded in a matrix of silica gel [24]. To derive the achievable performance of the sorption storage, the water-SWS equilibrium curves were measured as reported in [24], varying the temperature and water vapour pressure in a wide range of conditions. The obtained curves are useful to investigate the optimal operating conditions of the sorption TES. The sorption TES is strongly influenced by the discharging temperature, for this reason, an SH distribution system based on radiant floor was considered in the calculation, fixing the delivery temperature from 25 °C to 35 °C. The evaporation temperature was considered in a range between 5 °C and 15 °C, matching with winter ambient temperatures. Finally, the condensation temperature during charging is usually depending on the ambient temperature in summer, ranging from 25 °C to 35 °C. Starting from the above-reported fixed boundaries, to optimize the charging temperature level, the measured equilibrium curves were exploited to draw the operating cycle. Fig. 4 reports three different working cycles, at varying charging temperatures, in which the evaporation temperature was considered fixed at 10 °C (blue isobar in the graph), the condensation temperature was considered fixed at 35 °C (red isobar in the graph) and adsorption temperature to be delivered for SH was also fixed at 35 °C. The investigated charging temperatures were 80 °C, 85 °C, and 90 °C. As it can be argued, as long as the charging temperature was kept above 85 °C, the operation of the sorption TES was not affected, indeed the working cycle area is more or less unaffected and the amount of water vapour exchanged, which was directly linked to the achievable energy storage, passes from 42 wt%, at 85 °C, to 44 wt%, at 90 °C. Differently, when 80 °C charging temperature was considered, the uptake exchange dropped down to 25 wt%, and the area of the working cycle was reduced as well, thus limiting the overall energy storage capacity. According to this analysis, in this investigation a desorption temperature (charging) of 90 °C was considered, while ambient air was used as a heat sink to the condenser.

Based on the desired operating conditions of the sorption storage, in summer, solar heat was used to charge either, the sorption modules or the stratified water tank for DHW. Specifically, when solar energy was above a certain control threshold ($G_{min,STES}$), the sorption storage was charged at 90 °C. On the other hand, when solar energy was above the control threshold $G_{min,\ combi,S}$ the stratified water tank was charged at 65 °C. The solar heat, provided at the desorption temperature caused the desorption of the water vapour adsorbed onto the composite sorbent. The water vapour leaving the composite was condensed rejecting the

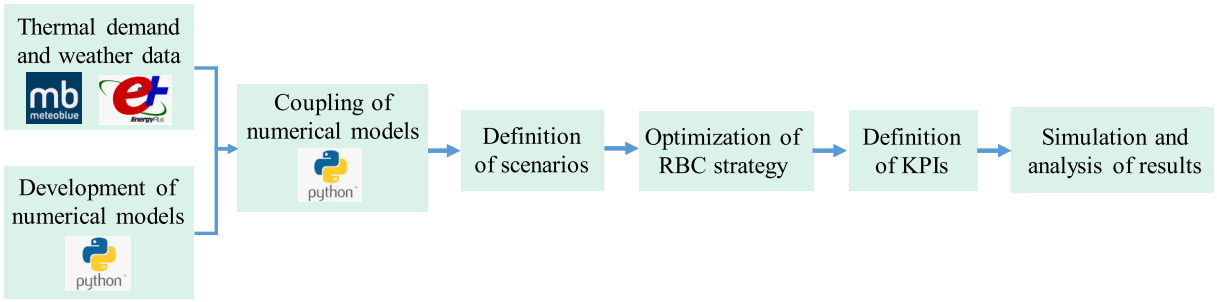

Fig. 1. Flowchart of the followed methodology.

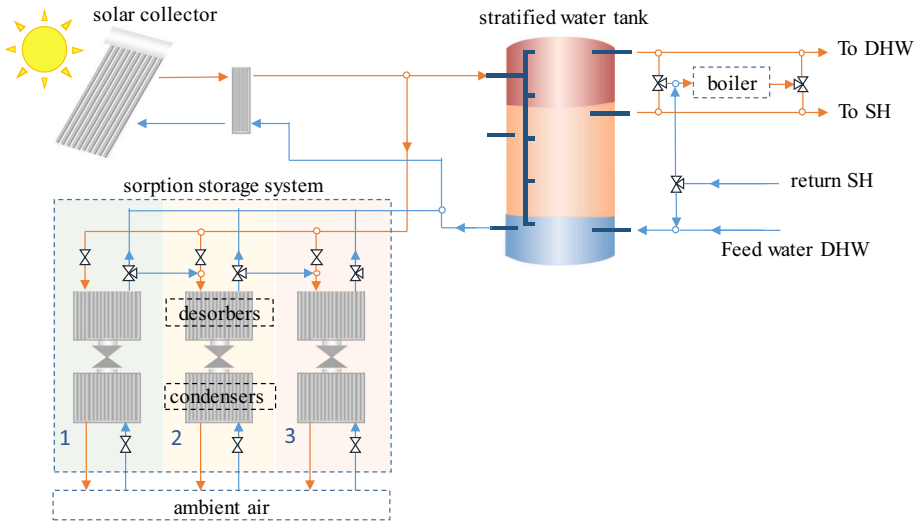

Fig. 2. System configuration in summer.

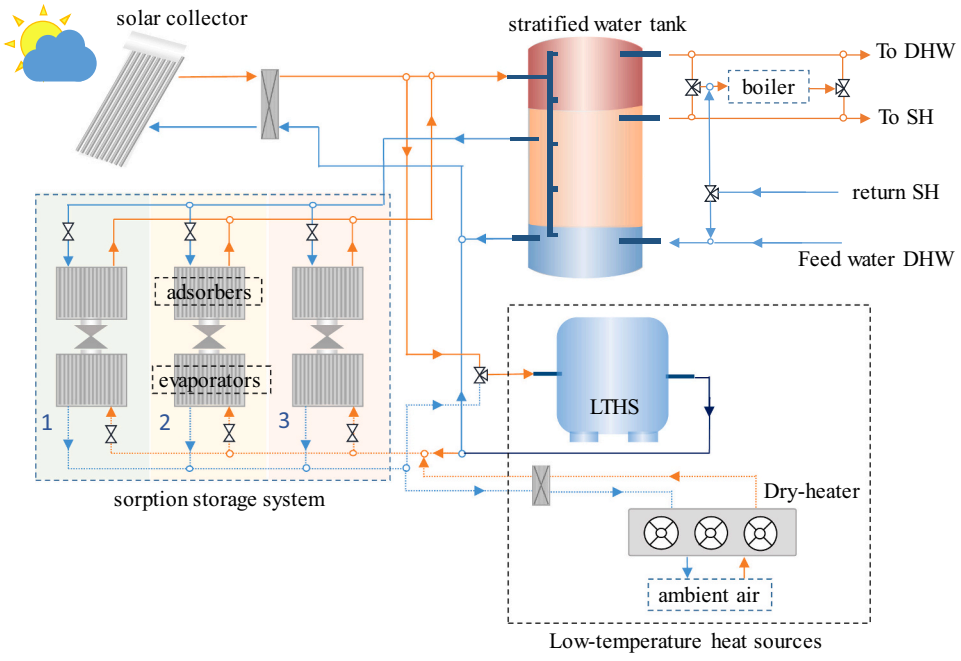

Fig. 3. System configuration in winter.

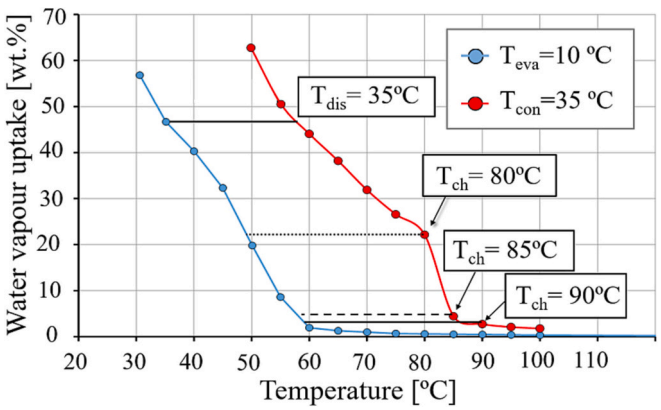

Fig. 4. w-t composite SWS-water equilibrium diagram, each equilibrium curve represents a different water vapour pressure.

condensation heat to the ambient.

The thermal power that a sorption module could adsorb during summer was limited by the kinetics reaction and the heat transfer rate driven by conduction inside the adsorber (i.e. the composite sorbent integrated into the heat exchanger) and many times was lower than the instantaneous solar power. For this reason, once the first active module was charged, the outgoing heat transfer fluid was used to heat up in series the next module, so the use of solar heat is maximized.

During winter (see Fig. 3), the system could charge the stratified water tank with solar heat for DHW (at 65 °C) or for SH (at around 35 °C) if the solar irradiation was above a certain threshold ($G_{min,combi,w}$). The stratified water tank could be also charged with heat of sorption (discharging the STES) to supply SH demand. Hot water from the stratified water tank was used to supply totally or partially (with support of the boiler) the thermal demand. Whenever SH demand was expected (for the next 24 h) and the middle part of the stratified water tank ($T_{combi,middle}$) was below its corresponding temperature threshold ($T_{combi,middle,set}$), the sorption system discharge was activated. The sorbent module was discharged to the stratified water tank once it had reached the required equilibrium temperature ($T_{sorb,set}$), which ranged from 25 to 35 °C (see Section 2.4.2). This temperature is a requirement to trigger the discharge of a sorption system and depends on the application, the sorption working cycle, and the sorbent material (see Fig. 4). To activate the adsorption process, the valve between the adsorber and the evaporator is opened, allowing the evaporation of the water and its adsorption in the sorbent material.

Indeed, the adsorption process needs a LTHS to assist the evaporator. The use of ambient air as a unique LTHS of a water-based sorption TES causes great system dependency on the ambient temperature and limitations in its operation especially during cold winter days, when SH is highly demanded. In the proposed system, to reduce the system dependency on ambient temperature, the evaporator was assisted by a low-temperature TES tank. In winter, whenever the low-temperature TES tank fell below the required temperature set point in the evaporator, it was charged at low temperature (20 °C) by the solar field if the solar irradiation was above the control threshold $G_{min,LTHS}$. Moreover, according to the system design, the stratified water tank could not receive hot water from the solar field and from the sorption storage simultaneously.

The system was assisted both in winter and summer by a backup natural gas boiler, whenever the stratified water tank was not at the required DHW or SH temperature set point when demanded. Hot water for DHW was supplied, either directly to the user or to the boiler, by the upper region of the stratified water tank. SH was supplied by the top of the middle region of the stratified tank. Return water entered at the bottom of the water tank. When the temperature at the top of the middle region of the combi tank fell below 20 °C, the SH circuit operated in a close loop with the boiler. Moreover, in case the boiler had a simultaneous demand of both SH and DHW, DHW was prioritized.

2.2. Input data: thermal demands and weather data

The solar-driven seasonal system under study must provide the SH and DHW demand needs of a 165 m^2 single-family house located in a cold climate. The location of Nuremberg (Germany) was selected to analyse the seasonal system since it presents relatively high solar irradiation in summer and low solar irradiation in winter, precisely when the SH is required by the occupants.

As shown in Fig. 5, the building has three floors however, just the first and second floors, with a surface of 67 m^2 each, were heated (the attic zone was not conditioned). A building model developed in OpenStudio [26] and simulated in Energyplus [27] was used to generate the SH consumption profiles. More information about the type of building, building temperature set points, etc. can be found in Crespo et al. [22]. The SH consumption profiles were generated with a simulation time-slot of 1 h. With regard to DHW, a consumption of 90 l/day [28] with a temperature rise from 10 to 60 °C was considered. The DHW temperature set point to deliver heat to the end user was set at 65 °C, since a temperature difference of 5 °C was assumed in the heat exchanger. An hourly-based time slot was first used to obtain the DHW consumption profiles, it was then interpolated to the first 15 min of every hour. The total thermal demand required by the building was 6990 kWh for SH and 1914 kWh for DHW.

Meteorological data [29] from different years of the location of Nuremberg, with a latitude of 49.4609° and a longitude of 11.0618°, was used to run the simulations.

2.3. Numerical model description

The performance of the different system scenarios was analysed through numerical simulations. The simulation of the seasonal energy system required knowing the response of each of its subcomponents under transient conditions. For this purpose, either physical models or performance maps of the subcomponents were considered. All physical models were implemented in Python [30] and are described in this section. The simulation of the whole system was also performed in Python considering a simulation time-step of 15 min.

2.3.1. Evacuated tube collectors

A 17.5 m^2 solar field composed of evacuated tube collectors AKOTEC

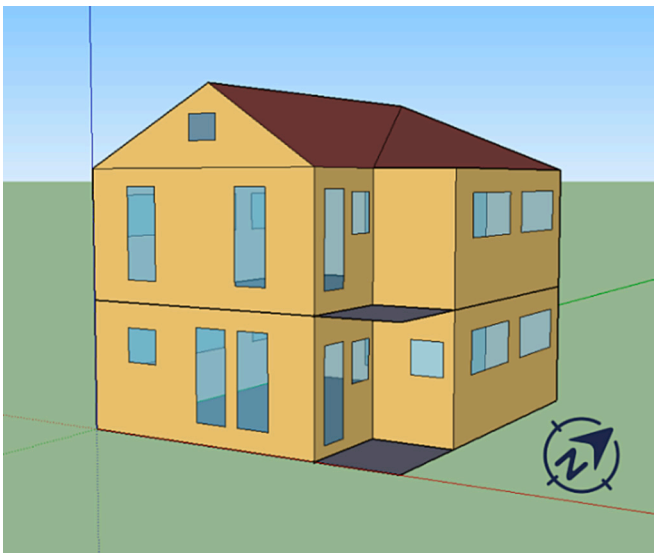

Fig. 5. Reference building considered in the study.

OEM Vario 3000–30 [31] with an aperture area of 4.46 m^2 was used for the simulations. The solar collectors were modelled using the energy balance equation of a general collector presented in Eq. (1).

$$IAM\ E_G\ A_{col}\ \eta_{overall} = \dot{m}_{col}\ C_p\ \left(T_{out,col} - T_{in,col}\right) \quad (1)$$

where IAM is the incidence angle modifier, E_G is the solar irradiation, and A_{col} is the area of collectors. The overall collector efficiency ($\eta_{overall}$) can be described as:

$$\eta_{overall} = a_0 - a_1\frac{T_{avg} - T_{amb}}{E_G} - a_2\frac{\left(T_{avg} - T_{amb}\right)^2}{E_G} \quad (2)$$

The energy balance was solved with an analytical approach. A detailed description of the physical model of the thermal collector and its validation can be found in Crespo et al. [22]. The thermal, optical, and operational parameters of the solar field are shown in Table 1.

The solar heat exchanger between the primary and the secondary loop was modelled using the epsilon-NTU method [34]. The heat transfer fluid in the solar collectors was water-glycol, while the secondary loop operated with water.

2.3.2. Stratified water tank

The heat coming either from the solar field or from the sorption storage was stored in a 1 m^3 constant volume stratified water tank. A 1D numerical model based on the finite control volume method was developed to analyse its thermal performance. 33 control volumes were considered; each control volume was considered fully mixed and was solved using an explicit scheme. The physical phenomena considered in the 1D model were: heat losses to the ambient, thermal conduction between nodes, and mass flow between nodes. A detailed description of the physical model of the stratified water tank and its validation can be found in Crespo et al. [22]. For controlling and performance analysis purposes, three sensors were set in the stratified water tank: at the upper part at 1.5 m ($T_{combi,top}$), at 0.75 m ($T_{combi,middle}$), and completely at the bottom ($T_{combi,bottom}$) part of the tank.

An internal time slot of 1 min was required to simulate the stratified water tank due to the ratio between node volume and inlet mass flow rate. A temperature of 25 °C was assumed as the initial condition. The thermal and physical parameters considered in the simulation are shown in Table 2.

2.3.3. Sorption storage tank

The sorption storage tank contained 20 modules of 100 kg of SWS, each of them composed of an adsorber/desorber (plate heat exchanger), an evaporator/condenser and its corresponding automatic valves. A detailed sketch of a sorption module coupled to the low-temperature heat storage, and to the dry-heater (winter configuration) is shown in Fig. 6.

The operation of the sorption modules was simulated using performance maps obtained by scaling up the results reported on the characterization of a lab-scale adsorber configuration reported in Mikhaeil et al. [23] and the equilibrium curves of SWS reported by Brancato et al. [36]. The performance maps provided the charging power (Q_{de}) and discharging power (Q_{ad}) as a function of the inlet temperature of the

Table 1
thermal, optimal and operational parameters of the solar field.

Parameter	Value	Parameter	Value
Total collector area, A_{col} (m^2)	17.5	Collectors' inclination	35°
Optical efficiency, a_0	0.559 [33]	Diffuse incidence angle modifier	1.314 [33]
First order efficiency, a_1 (W/m^2K)	1.485 [33]	Maximum pressure (bar)	10 [31]
Second order efficiency, a_2 (W/m^2K)	0.002 [33]	Specific heat (kJ/kgK)	3.9

Table 2
thermal, optimal and operational parameters of the solar field.

Parameter	Value	Parameter	Value
Top heat losses coefficient (W/m^2K)	0.32 [35]	Tank volume (m^3)	1
Edges heat losses coefficient (W/m^2K)	0.38 [35]	Tank height (m)	1.65
Bottom heat losses coefficient (W/m^2K)	2 [35]	HTF thermal conductivity (kJ/hmK)	2.14

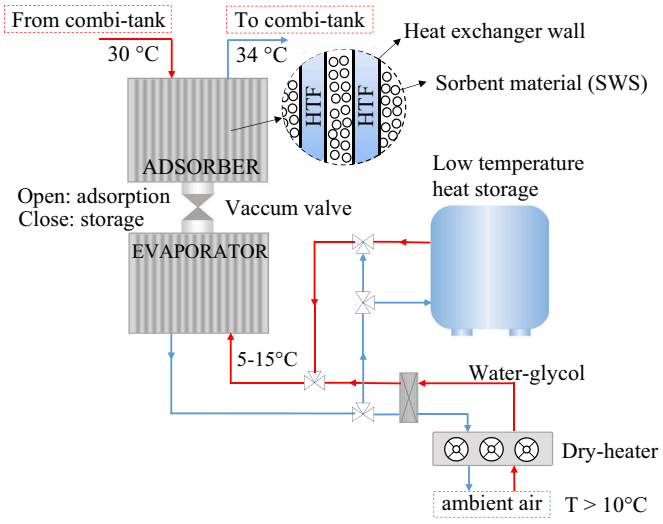

Fig. 6. Scheme of a sorption module and its corresponding low-temperature heat sources (temperatures correspond to the discharging process).

main components (adsorber, evaporator/condenser) of the sorption modules. The evaporator/condenser temperature was assumed equal to the inlet evaporator/condenser temperature during the discharging and charging process, respectively. The scaling-up was calculated for 100 kg of composite sorbent employing silica gel impregnated with 30 wt.\% of LiCl and considering the following constant mass flow rates: 720 kg/h in the absorber and desorber, 600 kg/h in the evaporator, and 900 kg/h in the condenser. According to the equilibrium thermodynamic curves reported in [24], each module containing silica gel and LiCl could store up to 30.5 kWh of energy, which summed up to 611 kWh for 20 modules. Moreover, to evaluate the evaporation power (Q_e) and condensation power (Q_c), as reported in Eqs. (3) and (4), an average ratio between adsorption enthalpy and water condensation/evaporation enthalpy equal to 1.2 was considered.

$$Q_e = \frac{Q_{de}}{1.2} = \dot{m}_e\ C_p\ \left(T_{in,e} - T_{out,e}\right) \quad (3)$$

$$Q_c = \frac{Q_{ad}}{1.2} = \dot{m}_c\ C_p\ \left(T_{out,c} - T_{in,c}\right) \quad (4)$$

During idle periods, the sorption modules comprising metal, water, and composite sorbent suffered heat losses through natural convection to the surroundings. For the sake of simplicity, some assumptions were considered: a constant ambient temperature for summer (21 °C) and winter (15 °C) was considered since the STES was located in a non-heated area, such as a garage or even buried underground. The STES was assumed as a lumped system with one control volume at a homogenous temperature. The temperature evolution was obtained considering the STES geometrical features, the equivalent heat capacity of the metal, sorbent material, and water, and a thermal insulation of glass wool of 5 cm of thickness in the lateral, bottom and top walls. Under these conditions, the temperature decrease of the sorption modules can be described by an exponential decay function [37], depending

on the convective heat transfer coefficient, external surface area, heat capacity, and the total thermal mass of the STES. Based on this approach, a performance map was generated to represent the heat losses along time for a module of 100 kg of SWS. Further details about the development of the performance maps and the SWS composite materials were reported in Crespo et al. [22] and Frazzica et al. [24], respectively.

Furthermore, for operational purposes, the state of charge (SoC) of the sorption heat storage system was calculated at every time-step. It was calculated as the average SoC of all the sorption modules. The SoC of one module during the charging process at every time step ($SoC^t_{ch,\ mod}$) was calculated as follows:

$$SoC^t_{ch,mod} = \frac{E^{t-1}_{stored} + E^t_{de}}{E_{max,mod}} \quad (5)$$

where $E_{max,\ mod}$ is the maximum storage capacity of one sorption module, E^{t-1}_{stored} is the sorption energy stored in the module and E^t_{de} is the sorption energy charged during the current time step. The SoC of one module during the discharging phase at each time step ($SoC^t_{dis,\ mod}$) was calculated using Eq. (6).

$$SoC^t_{dis,mod} = \frac{E^{t-1}_{stored} - E^t_{ad,sen} - E^t_{ad}}{E_{max,mod}} \quad (6)$$

where, $E^t_{ad,\ sen}$ is the sorption energy released by the module used to warm-up the reactor (sensible energy) at each time step and E^t_{ad} is the effective sorption energy released by the module to the stratified water tank at each time step. $E^t_{ad,\ sen}$ is equal to zero once the reactor is at the required sorption temperature and E^t_{ad} is equal to zero during the warming-up of the reactor.

2.3.4. Low-temperature heat source

Two LTHS could assist the evaporator: a buffer water tank and a dry-heater. The buffer water tank had a volume of 0.39 m^3. A 1D model of a water tank assuming one fully mixed control volume was considered in the simulations. Due to the short-term use of this storage tank, thermal losses to the surroundings were neglected.

Additionally, a dry-heater of 2.75 thermal kW assisted the evaporator of the sorption system during its discharge. The model of the dry-heater was based on an energy balance, which solved the equality between the Fourier's law of heat conduction [38] and the temperature gradient in the HTF fluid side of the heat exchanger. The energy balance is shown in Eq. (7), where the subscripts HTF corresponds to water with 15 % glycol. The average HTF temperature ($T_{avg,HTF}$) was assumed equal to the inlet HTF temperature of the dry heater. A UA value of 320 W/m^2K was considered in the simulations [39].

$$Q = \dot{m}\ C_{p,HTF}\ \left(T_{out,HTF} - T_{in,HTF}\right) = U\ A_{drycooler}\left(T_{amb} - T_{avg,HTF}\right) \quad (7)$$

2.3.5. Auxiliary subcomponents

A gas boiler of maximum thermal power of 9 kW and efficiency of 0.9 was considered in the simulations. The model of the gas boiler was based on the physical model type 122 presented in the Documentation of TRNSYS 18 [40].

The Reindl Model [41,42] was used to calculate the solar diffuse radiation on the tilted plane.

2.4. Enhanced system scenarios

Seasonal sorption TES systems coupled to a solar thermal field are very promising systems to supply SH demand in cold climates which present high temperatures and solar irradiations during the summer season. Sorbent materials for storage applications have shown very good properties, such as high energy density and low thermal losses. Nevertheless, the operation at system level and its implementation in a dwelling heating system must be further studied. The competitiveness of sorption TES against traditional fossil sources can be reached by optimizing the operation and identifying the best system configuration. In particular, the discharging process of the sorption modules is crucial to achieving interesting levels of efficiency which might push the technology to further integration into the building market.

2.4.1. Replacement of low temperature heat storage system

As previously mentioned, during the discharge, the water sorbent-based sorption system under study needs support from a LTHS, which ranges between 5 and 15 °C, depending on the weather conditions. According to the equilibrium curves of the SWS [24], as expected, the sorption storage system is more efficient at an evaporator temperature of 15 °C, rather than 5 °C, since the temperature lift between the heat source (evaporator) and the heat sink (adsorber) is reduced. In a previous study [22], considered as the benchmark in this study, a PCM tank [43] was used as the evaporator heat source, since PCM provide heat at a nearly constant temperature, 15 °C in this case (PCM melting temperature). The results indicated that the PCM storage tank was suitable for the application and allowed to discharge a high percentage of the STES system. Nevertheless, PCM has also some disadvantages, such as low thermal conductivity, subcooling, long-term stability [3], and high cost. Hence, the first proposed system modification of this study consists of replacing the PCM tank with a conventional water buffer tank with the same thermal capacity. This change entails that the HTF and the storage material are the same. Consequently, the efficiency of the low-temperature storage tank is higher, besides other advantages, such as its simplicity, easier integration, and lower cost compared with a PCM tank.

2.4.2. Variable temperature set-points of space heating and STES discharge

In the benchmark case, the supply SH set point temperature was constant and conservative (nominal value: 38 °C, see Fig. 7). The sorption storage was discharged when the temperature at the middle region of the combi-tank was below the same constant threshold. Consequently, the equilibrium temperature to be reached by the sorption modules was also constant (maximum SWS temperature: 35 °C). Therefore, during cold winter days, the system was always supported by the boiler to supply SH demand.

One of the main drawbacks of a seasonal sorption system containing SWS is the energy delivered to the adsorbent material in form of sensible heat to reach the adsorption temperature required to activate the thermo-chemical reaction. Having variable set point temperature (equilibrium temperatures) to discharge the SWS during autumn or winter days with relatively high ambient temperatures, allows SWS material to be heated up to lower temperatures in comparison with a constant and conservative discharging temperature set point. Furthermore, discharging the sorption TES at lower temperature reduces the temperature lift between the evaporator and the adsorber, achieving higher performance. Therefore, the next system modification proposed

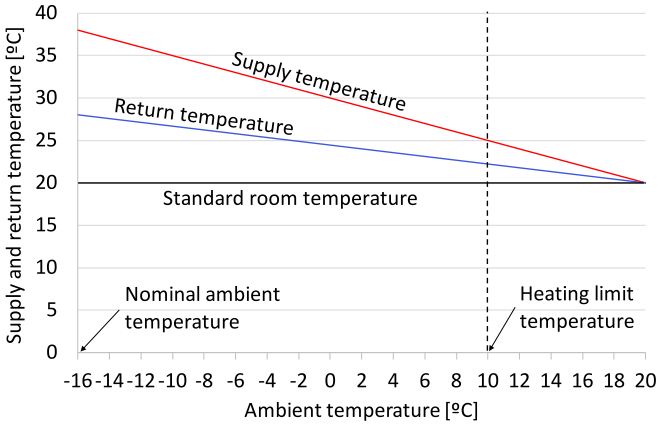

Fig. 7. SH temperature set-point based on ambient temperature [44].

in this study, consisted of setting a variable SH temperature set-point based on the ambient temperature. On the other hand, the equilibrium temperature to be reached by the sorption modules ($T_{sorb,set}$) and the temperature set point of the combi-tank ($T_{combi,middle,set}$) to trigger the discharge of the sorption storage could also vary based on the ambient temperature, or keep it constant at a nominal value. The higher the ambient temperature, the lower the SH supply set point temperature and the discharging set point temperature of the sorption modules if variable set points were considered.

2.4.3. Use of dry-heater during discharge

The last system modification consisted of the combination of a conventional dry-heater and a low-temperature heat storage (water buffer tank) to provide ambient heat to the evaporator. During winter days with relatively high ambient temperatures, the evaporator could receive heat from ambient air through the dry heater. On the other hand, during cold winter days, with very low ambient temperature, which matches with higher SH demands, the low-temperature heat storage (water buffer tank), charged by residual energy provided by the solar collectors' field, could assist the evaporator to discharge the STES. This approach aimed to extend the operation of the STES system and increase its efficiency.

2.4.4. Analysed scenarios

A total of 5 system scenarios were studied and compared: the benchmark presented by Crespo et al. [22] and four more scenarios which combine the different system and operational proposed modifications. The five scenarios and their particularities are presented in Table 3. Their thermal performance will be analysed and compared in the next section.

To delve into the influence of the LTHS on the sorption system efficiency, a scenario, in which the sorption storage has, whenever necessary, a heat source at 15 °C, was analysed. Furthermore, a parametrization analysis of the LTHS capacity was also performed. Both approaches were studied for the best-case scenario.

2.5. Control of the system

The seasonal energy system was operated with an RBC policy, which depended on the solar irradiation, ambient temperature, DHW and SH demands, sensors temperature in the stratified water tank (top, middle and bottom), temperature of the water buffer tank, and state of charge of the STES. Moreover, since the sorption storage needed warming up before discharge and its discharge was too slow for the SH needs, the SH demand for the next 24 h was also used as a state variable of the system. The RBC policy selected an operational mode based on the values at every time step of the afore-mentioned variables and the defined thresholds. The system could operate with more than 30 operational modes (the number of operational modes varied based on the analysed scenario as described in Subsection 2.4.4). The RBC policy followed the operation described in Section 2.1.

Crespo et al. [22] concluded that the control optimization of a solar-driven seasonal sorption TES system is crucial for its economic competitiveness against traditional heat sources. In this study, we carried out the control optimization of every proposed scenario. In this way, we could compare the different scenarios under optimal operational conditions. Since the system operation highly depended on solar energy availability, the following control thresholds were considered to optimize its operation:

1. Minimum solar irradiation in summer to charge the sorption storage tank ($G_{min,STES}$).
2. Minimum solar irradiation in summer to charge the stratified water tank ($G_{min,combi,S}$).
3. Minimum solar irradiation in winter to charge the stratified water tank ($G_{min,combi,W}$).
4. Minimum solar irradiation in winter to charge the low temperature heat source, either PCM tank or buffer water tank ($G_{min,LTHS}$).

The objective function of the system control optimization consisted of minimizing the total annual operational costs. The total annual operational cost was a cumulative reward, which consisted of (i) an economic penalty that was paid when the demand was not covered, (ii) the sum for every time step of the year of natural gas consumption of the boiler, and (iii) the electrical consumption of the pumps, and the dry-cooler (in the corresponding system approach). The only circumstance in which the end user demand cannot be fully covered occurred when there was simultaneous demand for DHW and SH and the water tank is below both set points. In that case, the SH demand could not be covered, and the system must pay a penalty. The equation of the total annual cost is shown in Eq. (6).

$$\text{Annual operational costs} = \sum_{t=0}^{J} \left[PF \left(E_{nosup,DHW} + E_{nosup,SH} \right) + C_{gas}\, E_b + C_{el}\, E_{el} \right] \tag{8}$$

As previously mentioned, an economic penalty was paid when the SH demand was not covered. A penalty factor of one time the gas price was assumed. A unitary cost for natural gas (C_{gas}) and electricity (C_{el}) of 61.5 €/MWh and 298 €/MWh [46], respectively (with taxes) was considered. A ratio of 0.085 [39] between thermal power provided by the dry-heater and fan electrical power consumption was considered to calculate its electricity consumption.

Further details about the optimization algorithm and its optimization parameters can be found in Crespo 2021 et al. [22]. Input data (weather data and thermal demand profiles) of the years 2010, 2011, and 2012 for the location of Nuremberg was used for the optimization. In that way, we ensured that the optimal control thresholds were applied to different sets of data. To analyse the system thermal performance once the thresholds have been selected, data from 2008 was used.

Table 3
proposed system scenarios and its corresponding operational set points.

Scenario	LTHS	SH supply temperature (T_{sh})	Temperature set point at the combi-tank to discharge the STES($T_{combi,middle,set}$)[a]	Equilibrium temperature set point ($T_{sorb,set}$)[a]
1 [22]	PCM tank	Constant	Constant	Constant
2	Water tank	Constant	Constant	Constant
3	Water tank	Function of T_{amb}	Function of T_{sh}	Function of T_{sh}
4	Water tank + dry-heater	Function of T_{amb}	Function of T_{sh}	Function of T_{sh}
5	Water tank	Function of T_{amb}	Constant	Constant

[a] See Section 2.1.

2.6. Definition of key performance indicators

This section presents the key performance indicators used to analyse the performance of the sorption storage system and of the overall energy system. The solar fraction (SF) indicates the amount of thermal demand supplied directly or indirectly by solar heat. The solar fraction can be calculated as follows:

$$SF = \frac{(D_{DHW} + D_{SH}) - E_b}{D_{DHW} + D_{SH}} \tag{9}$$

where, E_b is the share of the thermal demand supplied by the backup

boiler in one year, D_{DHW} is the annual DHW demand and D_{SH} is the annual SH demand.

The coefficient of performance of the sorption storage (COP), is a performance indicator commonly used by the authors to evaluate the efficiency of a sorption system. Its equation, presented in Eq. (10), consists of the ratio between the effective sorption energy released (E_{ad}) to the sum of the total energy consumed during the desorption, both sensible ($E_{de,sen}$) and sorption (E_{de}).

$$COP = \frac{E_{ad}}{E_{de,sen} + E_{de}} \tag{10}$$

If we focused on the discharging phase, the thermal performance of the STES can be expressed in energy terms by the discharging efficiency (η_{dis}). The discharging efficiency represents the ratio between the effective sorption energy released and the total energy consumed during the discharge, both sensible ($E_{ad,sen}$) and sorption.

$$\eta_{dis} = \frac{E_{ad}}{E_{ad,sen} + E_{ad}} \tag{11}$$

To compare the competitiveness between different type of TES system (sensible, latent, and thermo-chemical), especially in the residential sector where the space is very limited, the energy density is commonly used. Its expression is shown in Eq. (12).

$$e_d = \frac{E_{ad}}{V_{sorb}} \tag{12}$$

Although the volumetric energy density is commonly used by the authors to report the performance of TES systems, according to Fumey et al. [2], the volumetric energy density is not adequate for systems comparison due to the different testing conditions between studies. Therefore, those authors presented a new key performance indicator: the temperature effectiveness (TE), which focused on the ratio of resulting temperature gain in sorption compared to required temperature lift in desorption. In this study, also the TE was used to assess the temperature lift quality of sorption storage. The equations to calculate the average temperature effectiveness introduced by Fumey et al. are reported in Eqs. (13)–(15). The average evaporator and condenser temperatures ($T_{e,avg}$ and $T_{c,avg}$, respectively) were assumed equal to the average inlet temperatures at the evaporator and condenser, respectively.

$$TE_{avg} = \frac{GTL_{ad}}{GTL_{de}} \tag{13}$$

$$GTL_{ad} = T_{ad,avg} - T_{e,avg} \tag{14}$$

$$GTL_{de} = T_{de,avg} - T_{c,avg} \tag{15}$$

With regard to the environmental performance indicators, the CO_2 emissions were calculated by multiplying the annual thermal demand supplied by the solar system (without backup boiler), divided by the boiler efficiency, by the equivalent CO_2 emissions (0.18 kg/kWh) [45].

3. Results

3.1. Overall analysis for the different scenarios

Table 4 presents the key performance indicators for the studied scenarios. All results were obtained under optimal control policy, as indicated in the previous sections. $E_{primary}$ represents the primary energy consumption of the boiler, that is to say, the share of the thermal demand supplied by the boiler divided by the boiler efficiency. On the other hand, the term E_{coll} represents the thermal energy generated by the evacuated tube collectors. The optimal control thresholds for the five scenarios are shown in Table 5. A detail analysis of these results is presented in the upcoming sections.

3.2. Water tank as low temperature heat source

In the benchmark scenario (scenario 1 [22]), a PCM tank worked as LTHS of the sorption system. In scenario 2, a buffer water tank replaced the PCM tank: annual simulations indicated that the COP and the energy density of the sorption system increased 19.2 % (from 0.26 to 0.31) and 22.4 % (from 90.4 to 110.9 kWh/m^3). Using a water tank as LTHS allowed to have the same HTF and storage media. In consequence, the system would be simpler and would avoid an additional heat exchange between the storage media and the HTF, which decreases the system efficiency. Furthermore, by directly storing the solar heat in the water storage tank through the HTF, the temperature reached in the tank is slightly higher, which is beneficial, since the sorption system is more efficient at e.g. 15 °C than at 13 °C. Although using a water tank as low temperature heat source increased the sorption system COP by around 20 %, the annual operational cost of the whole seasonal energy system decreased by just a 0.7 %. The total capacity of the sorption system presented a low percentage of the total thermal demand. Therefore, an enhancement of the sorption COP affects slightly the total annual operational cost of the seasonal energy system. On the other hand, replacing a PCM tank with a water storage tank would reduce the investment costs.

3.2.1. Impact of variable temperature set-points

Scenario 3, in which the SH temperature set-point depended on ambient temperature, obtained a better solar fraction compared to scenario 2. In scenario 3 also the discharging temperature set-point of the sorption system depended on the ambient temperature. This means that, e.g. if the ambient temperature is 0 °C, the supply SH temperature is 30 °C (see Fig. 7). Hence, the discharge of the sorption system occurred when the material was at a minimum temperature of 33 °C (assuming a 3 °C of temperature difference in the heat exchanger). Thus, we avoided heating up the SWS up to 35 °C. On one hand, it may seem beneficial for the sorption system since we required less sensible energy to reach 33 °C than 35 °C. However, since the SH temperature set point was dependent on the ambient temperature, SH demand in scenario 3 could be many times directly supplied by the combi-tank, without the support of a backup boiler or energy from the sorption storage. This fact allowed to achieve a higher solar fraction of scenario 3 compared to

Table 5
Optimal control thresholds of the RBC strategy.

Scenario	2	3	4	5
$G_{min,STES}$ [W/m^2]	456	478	469	456
$G_{min,combi,S}$ [W/m^2]	136	142	121	147
$G_{min,combi,W}$ [W/m^2]	143	135	142	140
$G_{min,LTHS}$ [W/m^2]	100	100	100	100

Table 4
energetic KPI for the proposed system scenarios.

Scenario	$E_{primary}$ [kWh]	E_{coll} [kWh]	COP	$E_{de,sen}$ [kWh]	E_{de} [kWh]	E_{ad} [kWh]	SF [%]	e_d [kWh/m^3]	Use of STES [%]
1	6431.4	6075.4	0.26	692.7	547.8	325.5	34.99	90.4	87.7
2	6375.4	6115.6	0.31	706.4	578.9	399.2	35.50	110.9	92.8
3	6199.0	6198.1	0.29	690.1	532.5	349.2	37.3	97.0	85.2
4	6183.3	6186.3	0.30	697.7	537.1	371.6	37.5	103.2	86.8
5	6193.1	6200.1	0.30	700.8	572.4	383.0	37.4	106.4	93.7

scenario 2, but also caused more interruptions during the discharge of the sorption storage. The discharge of the sorption storage in scenario 3 was then limited to the coldest days, when the temperature at the middle part of the water tank was below the SH temperature set point. Therefore, the time elapsed between two consecutive discharges of the sorption system was greater in scenario 3 compared to scenario 2, which meant greater losses to the environment between two consecutive discharges, and consequently, more sensible energy supplied to reach the sorption temperature again. In consequence, the COP of scenario 2 was slightly higher than the one of scenario 3 (0.31 vs 0.29, respectively).

According to the sorption cycle, the sorption modules perform better at adsorption temperatures of 25 °C, rather than 35 °C, because of the higher temperature difference between regeneration and condensing temperature. Hence, the discharging efficiency in scenario 3 should be theoretically higher than for scenario 2. Nevertheless, this effect was overshadowed by the increase in thermal losses. In addition, by having lower SH set-points, a single discharge allowed to raise the temperature of the central part of the water tank enough to cover longer periods.

In contrast with scenario 3, in scenario 2, which presented a conservative and fixed SH temperature set point (38 °C), the sorption system needed to discharge several consecutive time-steps to reach the required temperature, obtaining a more continuous discharge and lower thermal losses between two consecutive discharges. In conclusion, for the studied location, the ambient temperature dependence on the discharge temperature set point of the sorption system was not beneficial for the discharging efficiency of the sorption system, as can be seen in Fig. 8 (scenario 3). Nevertheless, having a variable SH temperature set point based on ambient temperature was beneficial for the overall system solar fraction.

Higher solar fraction of scenario 3 caused lower annual operational costs compared to scenario 2, since, the back-up-boiler was required on fewer occasions. This behaviour is reflected in the reduction of the gas consumption shown in Table 6. As described in Section 2, if both SH and DHW demand required the use of the gas boiler, the DHW was prioritized, and the SH must be shortly switched off, which entails the payment of a penalty in the objective function. In this aspect, for the same reason already presented (SH demand is supplied directly from the water tank more time per year), scenario 3 allowed to reach a better thermal comfort for the users and reduced the penalty cost as shown in Table 6.

3.2.2. Impact of combined temperature set-points: variable and constant

Scenario 5 presented, as scenarios 3 and 4, the benefits of having a SH set point based on ambient temperature: the annual operational costs decreased in comparison with scenarios 1 and 2, and the thermal comfort of the user increased.

In Scenario 5 the sorption system was discharged at a constant temperature (35 °C), causing a slight increase in the COP (see Table 4) and in the discharging efficiency (see Fig. 8) compared to scenario 3. Nevertheless, the energy density of scenario 5 increased by 9 % in comparison with scenario 3. Supporting the results identified by comparing scenarios 2 and 3, having a constant, but slightly higher temperature set point to discharge the STES, allowed to have more continuous discharges, and less thermal losses to the ambient along the year. That conclusion is highly dependent on the ambient temperature and solar irradiation. The seasonal energy system must be studied in different locations to analyse the impact of weather conditions on the performance of the sorption system and on its thermal losses.

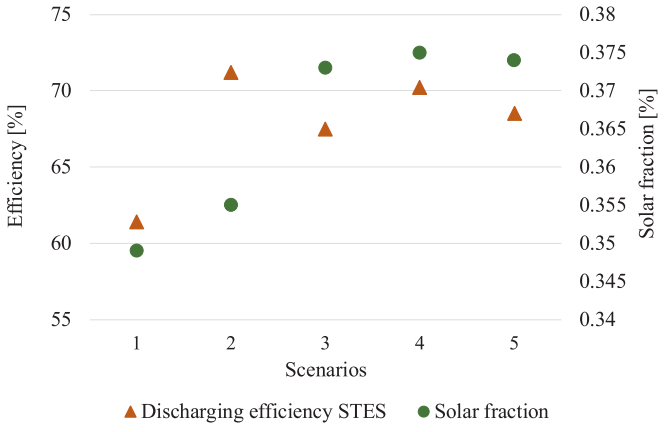

Fig. 8. discharging efficiency of STES vs solar fraction for the different studied scenarios.

Table 6
Breakdown of annual cost for every scenario.

Scenario	$Cost_{elect}$ [€]	Penalty [€]	$Cost_{gas}$ [€]	Total cost [€]
1	17.7	28.4	395.5	441.7
2	17.7	28.6	392.1	438.4
3	17.1	26.3	381.2	424.6
4	17.6	26.4	380.2	424.3
5	17.3	25.5	380.8	423.7

3.2.3. Dry-heater as low temperature heat source

During some cold winter days, the discharge process of the sorption system was interrupted since the LTHS required to assist the evaporator was not available (it was charged with solar heat). The implementation of a dry heater allowed to discharge the sorption system using ambient air as heat source. Nevertheless, for the case study, the dry-heater operated just for 9 h (per year), due to the low winter ambient temperatures in Nuremberg. Despite this fact, scenario 4 obtained slightly higher solar fraction, COP, energy density and discharging efficiency of the sorption system compared to scenario 3. Looking at the overall system level, the trade-off between solar fraction, and annual operational costs indicated that the integration of a dry-heater does not entail considerable improvements in the operational cost of the system that justifies its use. Therefore, the integration of a dry-heater for continental biogeographical regions [47] was not justified.

3.2.4. Overall performance comparison between scenarios

The operational differences between scenarios 3 and 5 showed the value of the seasonal concept of this study. Scenario 5 charged the STES more (93.6 %) compared to scenario 3 (87.1 %), causing that less solar energy was available to supply the DHW demand in summer and the increase in gas consumption in summer. However, due to the higher amount of solar heat stored in the form of heat of sorption during summer, the gas consumption during winter decreased compared to scenario 3. The total annual gas consumption of scenario 5 was lower compared to scenario 3 thanks to the seasonal behaviour of the sorption system.

Scenario 5 reached the best trade-off between minimization of annual operation costs and maximization of solar fraction and STES COP, which turns it into the most competitive scenario for the solar-driven seasonal sorption system. Scenario 5 presented a COP of 0.30 and an energy density of the sorption system of 106 kWh/m^3, calculated based on SWS volume. In this way, the value can be directly compared with the energy density at material level.

The CO_2 emissions savings in kg of CO_2 are 623.3, 633.4, 665.1, 668.0, and 666.2 for scenarios 1,2, 3, 4, and 5, respectively. The highest CO_2 savings were reached by scenario 4, due to the use of ambient air to discharge the sorption TES system. Indeed, as Fig. 9: depicts, scenario 4 presented more CO_2 emissions savings thanks to the use of the dry heater, even though the solar field generated less thermal energy compared to scenarios 3 and 5.

In this study, the economic sanctions due to the CO_2 emissions have not been considered. In a scenario where CO_2 emissions have a high cost, the interest in the technology could be even more justified and even the

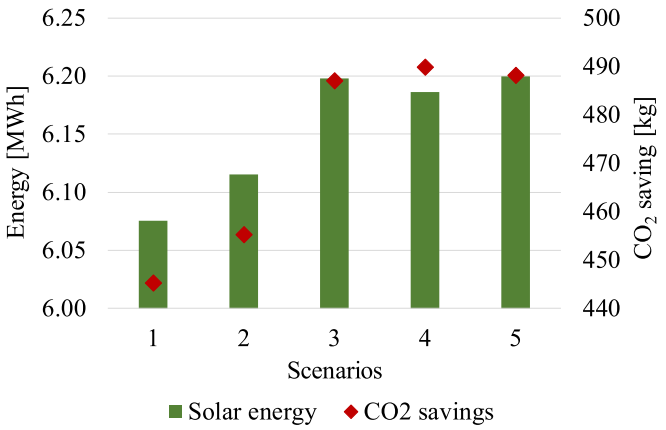

Fig. 9. Generated solar thermal energy and CO_2 savings.

implementation of the dry-heater could be debatable. Furthermore, the authors are aware that the gas and electricity costs are variable over time, which can affect the results reported in this study.

3.3. Best scenario

3.3.1. Overall analysis

Fig. 10 presents the monthly thermal energy, both DHW and SH, supplied by the whole energy system (without the boiler support) of scenario 5. From April to September, the system, in addition to supplying 90 % of the thermal demand, managed to charge the STES up to 93.6 %. From October to March, the seasonal energy system supplied 31 % of the thermal demand, taking advantage of both direct solar heat and heat of sorption.

In summer, during daily hours with high solar irradiation and high ambient temperature, solar heat was used to charge the sorption system. First, from 10:00 to 11:30, as shown in Fig. 11 (a), solar heat was just used to heat up the sorption module from 46 °C to 89 °C (T_{STES}). Considering that from the equilibrium point of view 90 °C was the optimal desorption temperature, accounting for a temperature difference needed to drive the process, 89 °C can be considered as a suitable inlet driving temperature for the charging stage. Hence, once the sorption module was at 89 °C, the sorption system was charged in form of heat of sorption (from 11.30 to 3 p.m). Indeed, the evolution of the SoC of the sorption system during a summer day in Nuremberg is presented on Fig. 11 (b). Once the desorption process finished, the temperature of the sorbent material started to decrease due to thermal losses to the ambient.

When the solar irradiation was not so intense, at the beginning and end of the day, solar heat was used to directly charge the stratified water tank, as shown in Fig. 11 (a). The average temperature of the stratified

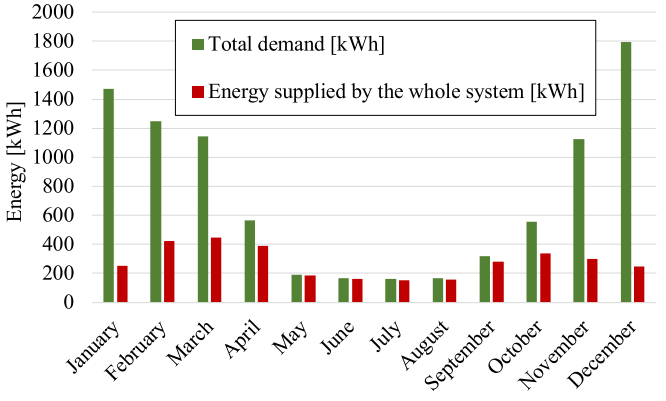

Fig. 10. monthly energy supplied by seasonal system vs total thermal demand.

water tank ($T_{combi,avg}$) increased in the morning hours (8 to 10 a.m) and at the end of the day (after 3 p.m). This heat was used for DHW.

Fig. 12 shows the evolution of the temperature at the middle part of the combi-tank ($T_{combi,middle}$) and its SoC for a winter day in Nuremberg. At around 4 a.m., when $T_{combi,middle}$ dropped below the set point (35 °C) and there was no solar irradiation that could charge the combi-tank, the sorption storage was discharged to increase the temperature of the combi-tank. That heat was immediately used to supply SH demand with the consequent decrease of the combi-tank temperature. From 13.00 to 18:00, solar heat was used to charge the combi-tank. Since the SH demand was zero during that period of the day, the temperature at the middle part of the combi-tank could reach 37 °C. Again, at the end of the day, the sorption storage was discharged to supply the SH demand. It is important to recall for this analysis, that the simulation time-step was 15 min.

Fumey et al. [2] compared several sorption-based long-term TES using the novel concept introduced by the author called temperature effectiveness. For comparison purposes with those sorption systems, the average temperature effectiveness of scenario 5 was calculated. The desorption was performed at 87.4 °C with a condensation temperature of 25.0 °C, obtaining a GTL_{de} of 62.3 °C. In winter, evaporation was performed at 13 °C, obtaining an average outlet temperature of 33 °C and reaching a GTL_{ad} of 20 °C. Hence, the average temperature effectiveness resulted in 0.33. The sorption system under study, filled with a selective water sorbent material, obtained a TE of 0.33 within the range of the closed fixed sorption TES systems reviewed by Fumery et al. [2], which ranged from 0.15 to 0.42. A TE of 0.33, as reported in a previous study [48], implies that a relatively low driving temperature was required to charge the sorption system. In contrast with other studies, which reported TE of 0.15, which means that concentrated collectors were required. Concentrated solar collectors are more expensive and, due to its higher weight, not suitable to be installed on a dwelling roof.

3.3.2. Detailed analysis of low temperature heat storage

In this section, a new scenario was analysed. The new scenario had the same operational temperature set points than scenario 5, however an infinite LTHS was considered instead of a water buffer tank charged by solar heat. Meaning that a low-temperature heat storage tank was always charged at 15 °C to provide heat to the evaporator of the sorption modules. Under this assumption, the sorption storage system was discharged in just one month and a half, as shown in Fig. 13, instead of the 5 months required by scenario 5. The sorption storage using an infinite LTHS operated with fewer interruptions during its discharge, obtained a COP, a discharging efficiency, and an energy density of 0.39, 90 %, and 139 kWh/m^3, respectively, resulting in a 24, 26, and 23 % improvement with respect to the scenario 5.

Furthermore, scenario 5 was simulated under different sizes of low temperature heat source (always under optimal control settings). The improvement, both economically and energetically, due to the increase in the LTHS volume was minimal or even non-existent, as reported in Table 7.

In conclusion, the results indicated that the thermal performance of the sorption TES system is limited by unavailability of the LTHS and not by the size of the latter one. Indeed, low solar irradiation during winter prevents a continuous discharge of the sorption modules.

4. Conclusions

In this study different scenarios to enhance the thermal performance and solar fraction of a solar-driven seasonal sorption storage system were analysed. The enhancements consisted of different system and operational modifications to increase the discharging efficiency of the novel water-based sorption system or the overall solar fraction. All scenarios were analysed under an optimal RBC control policy and for one whole year to analyse the effect of the storage system between seasons. The goal of the seasonal heating system was to supply DHW and

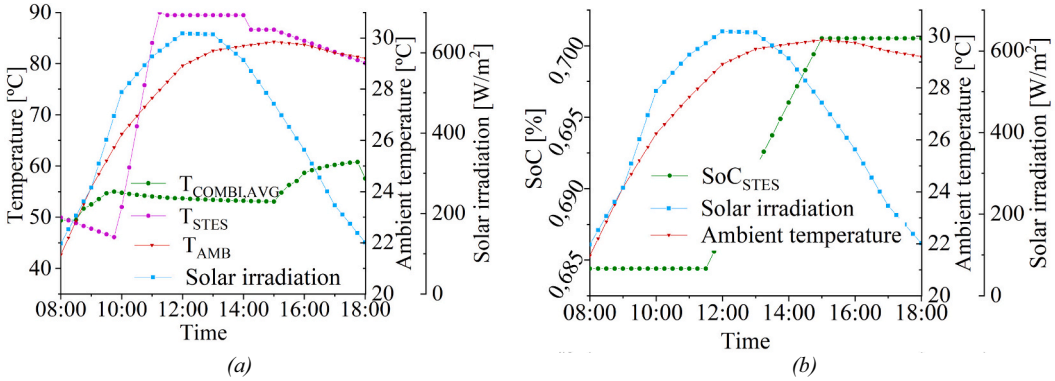

Fig. 11. Evolution of system and meteorological variables during the charging process on a hot summer day (29/07/2008). Temperatures of the combi-tank and sorption storage (a). State of charge of the sorption storage (b).

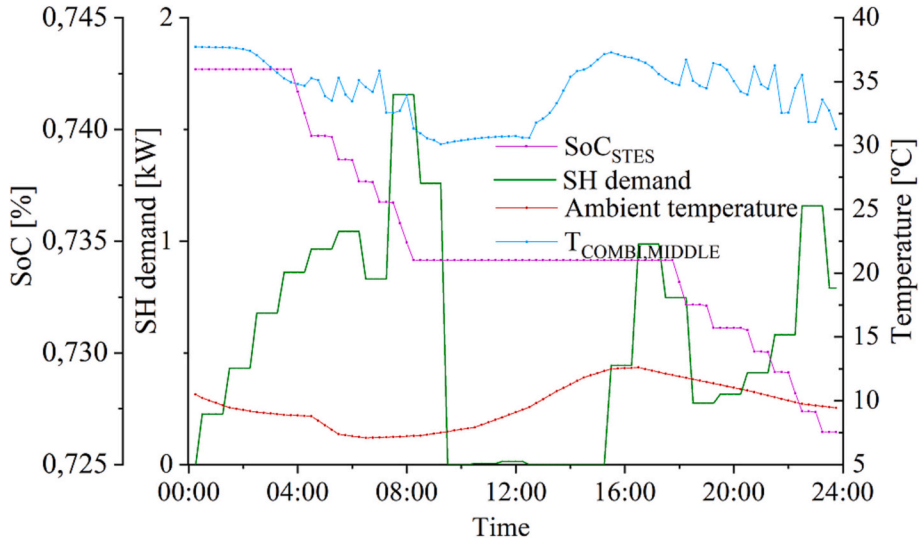

Fig. 12. Evolution of some system variables during discharging process on a cold winter day (04/11/2008).

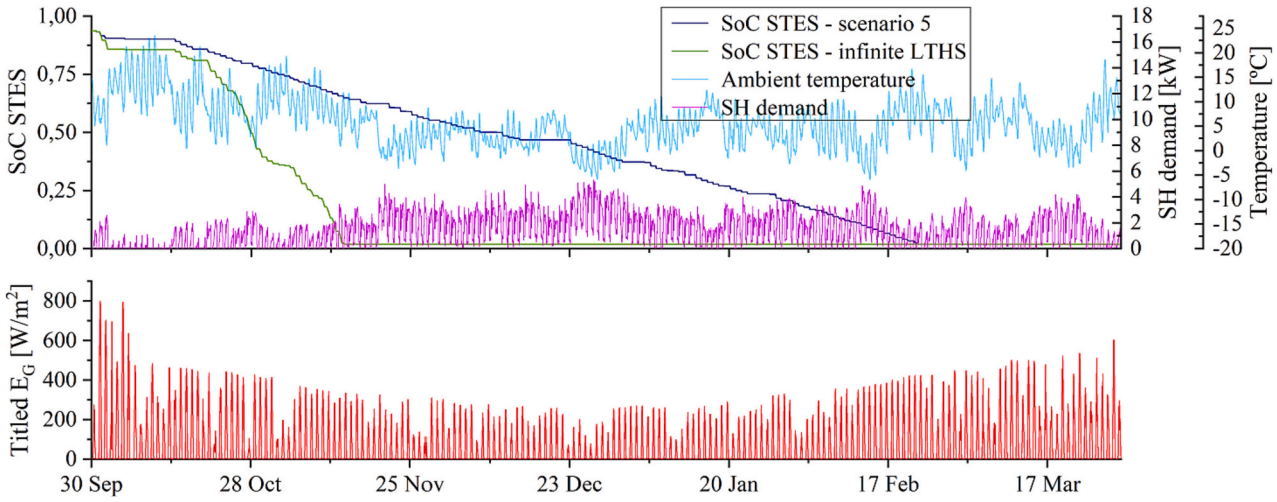

Fig. 13. Evolution of the state of charge of the sorption storage system during winter for scenario 5 and a scenario with infinite LTHS.

SH to a single-family house in a cold climatic region. The main results obtained in this study are:

- The use of a water tank as low-temperature heat source to assist the evaporator of the sorption system allowed to obtain higher COP and energy density (increase of 19.2 % and 22.4 %, respectively) compared to a latent heat energy storage tank. Phase changed

Table 7
Results of the KPIs for different LTHS volumes under the conditions of scenario 5.

LTHS size (litres)	Total annual costs (€)	SF (%)	COP_{STES}
300	425.2	37.2	0.29
390 (original)	423.7	37.4	0.30
500	423.5	37.4	0.29
600	423.2	37.4	0.29

materials have low thermal conductivity and are commonly expensive. Hence, using water as storage medium instead of PCM, allows the HTF and the storage medium to be the same, enhancing the system efficiency and reducing the investment costs.

- The ambient temperature dependence on the temperature set point of the combi-tank that trigger the discharge of the sorption system was not beneficial for its discharging efficiency, energy density, and COP. Having a fixed and more conservative discharging temperature set point (35 °C) allowed, among other aspects, to have fewer pauses between two consecutive discharges and therefore, less thermal losses to the ambient. Thus, the energy density was increased by 9 %.
- The integration of a dry-heater as low-temperature heat source into a seasonal water-based sorption system to be operated in a cold climate region was not justified (as it was used for a few hours in a year). Both, the slight increase in solar fraction and in annual operational costs did not compensate for the investment cost of the dry-heater. Nevertheless, in this study, the economic sanctions due to the CO_2 emissions were not considered. In a scenario where CO_2 emissions would have an impact in the cost, the implementation of the dry-heater could be debatable.
- The energy density of a water-based seasonal sorption system driven by solar energy highly depended on the weather conditions (ambient temperature and solar irradiation, and on the type of low-temperature source). The energy density of the seasonal sorption TES could increase by 23 % if a constant heat source (i.e. industrial waste heat or geothermal energy) could be used to assist the evaporator instead of relying on solar energy availability during winter. To a lesser extent, the efficiency of the sorption storage was affected by its discharging temperature set point.
- A seasonal water-based sorption system driven by solar thermal collectors integrated into a nearly zero emissions (NZE) single-family house located in a cold region supplied 37.4 % of the total thermal demand. The sorption system composed by 20 modules of LiCl-silica gel obtained a COP of 0.3, an energy density of 106 kWh/m^3 and a temperature effectiveness of 0.33 as optimal results.
- The seasonal sorption system must be analysed in different locations in future work to validate its feasibility in different climates.

Declaration of competing interest

The authors declare the following financial interests/personal relationships which may be considered as potential competing interests: Alicia Crespo reports financial support was provided by Spain Ministry of Science and Innovation. Cesar Fernandez reports financial support was provided by Spain Ministry of Science and Innovation. Alicia Crespo reports financial support was provided by Government of Catalonia Agency for Administration of University and Research Grants. Alvaro de Gracia reports financial support was provided by Serra Hunter.

Data availability

Data will be made available on request.

Acknowledgements

This work was partially funded by the Ministerio de Ciencia e Innovación - Agencia Estatal de Investigación (PID2021-123511OB-C31 - MCIN/AEI/10.13039/501100011033/FEDER, EU) and by the Ministerio de Ciencia, Innovación y Universidades—Agencia Estatal de Investigación (AEI) (RED2018-102431-T). This work is partially supported by ICREA under the ICREA Academia programme. The authors would also like to thank the Catalan Government for the quality accreditation given to their research group (2017 SGR 1537). GREiA is certified agent TECNIO in the category of technology developers from the Government of Catalonia. Alicia Crespo would also like to acknowledge the financial support of the FI-SDUR grant from the AGAUR of the Generalitat de Catalunya and Secretaria d'Universitats i Recerca del Departament d'Empresa i Coneix-ement de la Generalitat de Catalunya. Alvaro de Gracia wants to thank the Serra Hunter Programme for its position at University of Lleida.

References

[1] IEA, Heating, Available online:, IEA, Paris, 2021 https://www.iea.org/reports/heating.
[2] B. Fumey, R. Weber, L. Baldini, Sorption based long-term thermal energy storage – process classification and analysis of performance limitations: a review, Renew. Sust. Energ. Rev. 111 (2019) 57–74, https://doi.org/10.1016/j.rser.2019.05.006.
[3] L.F. Cabeza (Ed.), Advances in thermal energy storage systems - Methods and Applications, 2nd Edition, Woodhead Publishing, 2020. ISBN 9780128198858.
[4] H.A. Zondag, Sorption heat storage - Chapter 6, in: Solar Energy Storage, 2015.
[5] J. Jänchen, D. Ackermann, H. Stach, W. Brösicke, Studies of the water adsorption on zeolites and modified mesoporous materials for seasonal storage of solar heat, Sol. Energy 76 (2004) 339–344, https://doi.org/10.1016/j.solener.2003.07.036.
[6] S.P. Casey, J. Elvins, S. Riffat, A. Robinson, Salt impregnated desiccant matrices for 'open' thermochemical energy storage—selection, synthesis and characterisation of candidate materials, Energy Build. 84 (2014) 412–425, https://doi.org/10.1016/j.enbuild.2014.08.028.
[7] M.-M. Druske, A. Fopah-Lele, K. Korhammer, H.U. Rammelberg, N. Wegscheider, W. Ruck, T. Schmidt, Developed materials for thermal energy storage: synthesis and characterization, Energy Procedia 61 (2014) 96–99, https://doi.org/10.1016/j.egypro.2014.11.915.
[8] H. Liu, K. Nagano, J. Togawa, A composite material made of mesoporous siliceous shale impregnated with lithium chloride for an open sorption thermal energy storage system, Sol. Energy 111 (2015) 186–200, https://doi.org/10.1016/j.solener.2014.10.044.
[9] L. Jiang, R.Z. Wang, L.W. Wang, A.P. Roskilly, Investigation on an innovative resorption system for seasonal thermal energy storage, Energy Convers. Manag. 149 (2017) 129–139, https://doi.org/10.1016/j.enconman.2017.07.018.
[10] K.E. N'Tsoukpoe, F. Kuznik, A reality check on long-term thermochemical heat storage for household applications, Renew. Sust. Energ. Rev. 139 (2021), https://doi.org/10.1016/j.rser.2020.110683.
[11] T.X. Li, S. Wu, T. Yan, R.Z. Wang, J. Zhu, Experimental investigation on a dual-mode thermochemical sorption energy storage system, Energy 140 (2017) 383–394, https://doi.org/10.1016/j.energy.2017.08.073.
[12] T. Li, R. Wang, J.K. Kiplagat, Y.T. Kang, Performance analysis of an integrated energy storage and energy upgrade thermochemical solid-gas sorption system for seasonal storage of solar thermal energy, Energy 50 (2013) 454–467, https://doi.org/10.1016/j.energy.2012.11.043.
[13] L. Jiang, S. Li, R.Q. Wang, Y.B. Fan, X.J. Zhang, A.P. Roskilly, Performance analysis on a hybrid compression-assisted sorption thermal battery for seasonal heat storage in severe cold region, Renew. Energy 180 (2021) 398–409, https://doi.org/10.1016/j.renene.2021.08.101.
[14] L. Jiang, W. Liu, Y.C. Lin, R.Q. Wang, X.J. Zhang, M.K. Hu, Hybrid thermochemical sorption seasonal storage for ultra-low temperature solar energy utilization, Energy 239 (2022), https://doi.org/10.1016/j.energy.2021.122068.
[15] Z. Ma, H. Bao, A.P. Roskilly, Electricity-assisted thermochemical sorption system for seasonal solar energy storage, Energy Convers. Manag. 209 (2020), 112659, https://doi.org/10.1016/j.enconman.2020.112659.
[16] Z. Ma, H. Bao, A.P. Roskilly, Seasonal solar thermal energy storage using thermochemical sorption in domestic dwellings in the UK, Energy 166 (2019) 213–222, https://doi.org/10.1016/j.energy.2018.10.066.
[17] A. Frazzica, A. Freni, Adsorbent working pairs for solar thermal energy storage in buildings, Renew. Energy 110 (2017) 87–94, https://doi.org/10.1016/j.renene.2016.09.047.
[18] A. Frazzica, V. Brancato, B. Dawoud, Unified methodology to identify the potential application of seasonal sorption storage technology, Energies 13 (2020), https://doi.org/10.3390/en13051037.
[19] S. Mauran, H. Lahmidi, V. Goetz, Solar heating and cooling by a thermochemical process. First experiments of a prototype storing 60 kW h by a solid/gas reaction, Sol. Energy 82 (2008) 623–636, https://doi.org/10.1016/j.solener.2008.01.002.
[20] Y.J. Zhao, R.Z. Wang, Y.N. Zhang, N. Yu, Development of SrBr 2 composite sorbents for a sorption thermal energy storage system to store low-temperature heat, Energy 115 (2016) 129–139, https://doi.org/10.1016/j.energy.2016.09.013.
[21] N. Yu, R.Z. Wang, L.W. Wang, Theoretical and experimental investigation of a closed sorption thermal storage prototype using LiCl/water, Energy 93 (2015) 1523–1534, https://doi.org/10.1016/j.energy.2015.10.001.

[22] A. Crespo, C. Fernández, D. Vérez, J. Tarragona, E. Borri, A. Frazzica, L.F. Cabeza, A. de Gracia, Thermal performance assessment and control optimization of a solar-driven seasonal sorption storage system for residential application, Energy 263 (2023), 125382, https://doi.org/10.1016/j.energy.2022.125382.
[23] M. Mikhaeil, M. Gaderer, B. Dawoud, On the development of an innovative adsorber plate heat exchanger for adsorption heat transformation processes; an experimental and numerical study, Energy 207 (2020), 118272, https://doi.org/10.1016/j.energy.2020.118272.
[24] A. Frazzica, V. Brancato, A. Caprì, C. Cannilla, L.G. Gordeeva, Y.I. Aristov, Development of "salt in porous matrix" composites based on LiCl for sorption thermal energy storage, Energy 208 (2020), 118338, https://doi.org/10.1016/j.energy.2020.118338.
[25] G. Engel, S. Asenbeck, R. Köll, H. Kerskes, W. Wagner, W. van Helden, Simulation of a seasonal, solar-driven sorption storage heating system, J. Energy Storage 13 (2017) 40–47, https://doi.org/10.1016/j.est.2017.06.001.
[26] R. Guglielmetti, D. Macumber, N. Long, OpenStudio: An Open Source Integrated Analysis Platform. Proc. Build. Simulation, Sydney, Aust, 2011 doi:Preprint NREL/CP-5500-51836.
[27] D.B. Crawley, L.K. Lawrie, F.C. Winkelmann, W.F. Buhl, Y.J. Huang, C.O. Pedersen, R.K. Strand, R.J. Liesen, D.E. Fisher, M.J. Witte, et al., EnergyPlus: creating a new-generation building energy simulation program, Energy Build. 33 (2001) 319–331, https://doi.org/10.1016/S0378-7788(00)00114-6.
[28] University of Perugia, D5.3 Dynamic User-building Interaction Model Predicting Thermal-energy Behaviour - Technical Report of SWS-heating Project, 2019.
[29] Meteoblue AG, Available online: https://content.meteoblue.com/en (accessed on Nov 10, 2020).
[30] Y. Shevchuk, NeuPy - Neural Networks in Python, Available online: http://neupy.com/2016/12/17/hyperparameter_optimization_for_neural_networks.html#tree-structured-parzen-estimators-tpe (last accessed: 02.02.2021).
[31] TÜVRheinland, Solar KEYMARK Certificate - Licence Number: 011-7S660R of the Collector OEM Vario 3000-30 hp of Akotec Produktionsgesellschaft GmbH, 2013.
[33] University of Lleida, National Technical University of Athens, Istituto di Tecnologie Avanzate per l'Energia, C. D5.1 Optimised System Control and Strategies. Tech. Reports SWS-heating Proj, 2020.
[34] Y.A. Cengel, Heat Transfer: A Practical Approach, 2nd edition, McGraw-Hill, New York, 2002, ISBN 978-0072458930.
[35] D. Vérez, E. Borri, A. Crespo, G. Zsembinszki, B. Dawoud, L.F. Cabeza, Experimental study of a small-size vacuum insulated water tank for building applications, Sustain. 13 (2021) 1–11, https://doi.org/10.3390/su13105329.
[36] V. Brancato, A. Frazzica, A. Caprì, L. Gordeeva, Y. Aristov, M. Mikhaeil, B. Dawoud, SWS composites based on LiCl for sorption thermal energy storage: thermochemical and kinetic properties, Available online:, in: ENERSTOCK 2021. Ljubljana, 2021.
[37] Y.A. Çengel, A. Ghajar, in: M. Hill (Ed.), Heat and Mass Transfer: Fundamentals and Applications, 5th edition, 2015.
[38] J.P. Holman, Heat Transfer, 10th edition, 2009, ISBN 978-0073529363.
[39] Roen Est Group, Available online: https://www.roenest.com/download/ (accessed on Nov 10, 2021).
[40] S.A. Klein, et al., TRNSYS 18: A Transient System Simulation Program, 2017.
[41] D.T. Reindl, W.A. Beckamnn, Diffuse fraction correlations, Sol. Energy 45 (1990) 1–7.
[42] D.T. Reindl, W.A. Beckamnn, Evaluation of hourly tilted surface radiation models, Sol. Energy 45 (1990) 9–17.
[43] A. Crespo, G. Zsembinszki, D. Vérez, E. Borri, C. Fernández, L.F. Cabeza, A. de Gracia, Optimization of design variables of a phase change material storage tank and comparison of a 2d implicit vs. 2d explicit model, Energies 14 (2021), https://doi.org/10.3390/en14092605.
[44] Ostbayerische Technische Hochschule Regensburg (OTH), Deliverable 3.1: "Requirements for the Sysnthesis of Sorbent Materials" - EU H2020 SWS-Heating, 2018.
[45] Catalan Office of Climate Change, Practical guide for calculating greenhouse has (ghg) emissions, Available online: https://canviclimatic.gencat.cat/web/.content/04_ACTUA/Com_calcular_emissions_GEH/guia_de_calcul_demissions_de_co2/190301_Practical-guide-calculating-GHG-emissions_OCCC.pdf (accessed on Apr 1, 2022).
[46] Technical report; Bundesnetzagentur; Bundeskartellamt. Monitoring report 2017 - key findings, Available online: https://www.bundesnetzagentur.de/.
[47] Biogeographic regions in Europe, Available online: https://www.eea.europa.eu/data-and-maps/figures/biogeographical-regions-in-europe-1 (last accessed: 02.02.2021).
[48] A. Crespo, A.De Gracia, A. Frazzica, Solar-driven Sorption System for Seasonal Heat Storage Under Optimal Control: Study for Different Climatic Zones, 2022.